Pediatric Radiology (2020) 50:1959–1973
https://doi.org/10.1007/s00247-020-04777-z

FETAL IMAGING

# Imaging of fetal brain tumors

Patricia Cornejo[1,2,3,4,5] · Tamara Feygin[6] · Jennifer Vaughn[1,2,3,5] · Cory M. Pfeifer[7] · Alexandra Korostyshevska[8] · Mittun Patel[1,3,5] · Dianna M. E. Bardo[1,2,3,4,5] · Jeffrey Miller[1,2,3,4,5] · Luis F. Goncalves[1,3,5]

Received: 29 November 2019 / Revised: 13 May 2020 / Accepted: 8 July 2020 / Published online: 19 November 2020


## Abstract

Congenital brain tumors, defined as those diagnosed prenatally or within the first 2 months of age, represent less than 2% of pediatric brain tumors. Their location, prevalence and pathophysiology differ from those of tumors that develop later in life. Imaging plays a crucial role in diagnosis, tumor characterization and treatment planning. The most common lesions diagnosed in utero are teratomas, followed by gliomas, choroid plexus papillomas and craniopharyngiomas. In this review, we summarize the pathogenesis, diagnosis, management and prognosis of the most frequent fetal brain tumors.

**Keywords** Brain · Congenital · Fetus · Magnetic resonance imaging · Tumor · Ultrasonography

## Introduction

Prenatal diagnosis of fetal neoplasms has increased over the last few decades as a direct result of continuous advances in fetal imaging [1–6]. Despite this trend, timely and accurate diagnosis remains challenging for several reasons. First, congenital neoplasms are rare, with a reported incidence for all tumors ranging 1.7–13.5 per 100,000 live births [1, 2]; the true incidence might be underestimated because cases of fetal demise, miscarriage and pregnancy termination tend to be underreported. Second, congenital tumors often differ histologically, pathophysiologically and in imaging appearance from tumors that develop later in life [1, 6–8]. Third, most of the information available about congenital tumors is based on postnatal imaging following symptomatic presentation after birth because the majority of these lesions do not cause signs and symptoms during pregnancy that would warrant additional obstetric imaging.

Congenital brain tumors are even more rare compared to body tumors, accounting for 0.5% to 1.9% of all pediatric tumors [4, 5]. Most are incidentally diagnosed by prenatal US during the second or third trimester. Thus, the limited literature available on congenital brain tumors comprises mainly case reports. To complicate matters, the imaging features of the more prevalent non-neoplastic central nervous system (CNS) anomalies, i.e. lipomas and hemorrhage, overlap considerably with those of congenital brain tumors because these lesions can demonstrate mass effect on adjacent structures, raising concern for neoplasm.

Fetal tumors can be histologically benign or malignant; however, their prognosis tends to be poor, especially for intracranial lesions. This is largely related to their unique pathogenesis, which is characterized by embryonic cell differentiation with a very high mitotic rate and impactful tumor volumes. Occasionally, even a benign intracranial neoplasm produces significant complications, for example through mass effect or secondary to hypermetabolism.

✉ Patricia Cornejo
pcornejo@phoenixchildrens.com

1 Department of Radiology, Phoenix Children's Hospital, 1919 E. Thomas Road, Phoenix, AZ 85016, USA

2 Department of Neuroradiology, Barrows Neurological Institute, Phoenix, AZ, USA

3 Department of Radiology, University of Arizona College of Medicine, Phoenix, AZ, USA

4 Department of Radiology, Mayo Clinic Arizona, Phoenix, AZ, USA

5 Department of Radiology, Creighton University School of Medicine, Phoenix, AZ, USA

6 Department of Radiology, The Children's Hospital of Philadelphia, Philadelphia, PA, USA

7 Department of Radiology, UT Southwestern, Dallas, TX, USA

8 International Tomography Center of the Siberian Branch of the Russian Academy of Sciences, Novosibirsk, Russian Federation

Akin to brain tumors presenting during the first year of age, about 70% of fetal brain tumors are supratentorial [4–6]. Masses can be intra- or extra-axial, occasionally growing to such a large size that anatomical landmarks become markedly distorted and determining the site of origin is almost impossible. Intracranial teratomas account for approximately half of cases, followed by astrocytomas, choroid plexus papillomas, craniopharyngiomas and tumors of embryonal origin such as medulloblastomas and atypical teratoid/rhabdoid tumors (ATRT) [1, 6, 9]. Congenital tumors of ependymal, meningeal and mesenchymal origins are less frequent [4, 10–16]. The final diagnosis is made by histopathological evaluation, molecular analyses or complex genetic testing.

Early and accurate diagnosis of fetal tumors significantly influences pregnancy management and delivery planning. Multimodality imaging plays an important role in the diagnosis of fetal tumors and evaluation of their resultant complications. The diagnosis of an intracranial mass on obstetric US should prompt further evaluation by prenatal MRI. Depending on the tumor location, a reasonable differential diagnosis can be made (Table 1). Detailed assessment can be performed using a variety of MR sequences designed to depict lesion morphology, with careful search for calcifications, blood products and fat deposits [1, 4]. New MR sequences can also aid in the evaluation of fetal brain tumors. These include diffusion-weighted imaging, which provides quantification of a lesion's diffusivity, and volumetric MR imaging, which can accurately estimate mass volume [17]. The recent introduction of macromolecular proton factor mapping techniques to fetal imaging, which use unbiased quantitative data comparison [18, 19], are promising for quantitative tissue characterization.

Last but not least, it is important to remember that certain brain tumors can be the initial manifestation of more complex tumor predisposition syndromes or genetic disarrangements (Table 2). In these cases, a meticulous search of additional fetal anomalies is crucial for prenatal–postnatal management and parental counseling.

The first attempts to provide a curative prenatal treatment or prevent lethal complications were introduced during the 1980s [20]. While several case reports and series describe successful intrauterine treatment for a few types of fetal tumors, mainly sacrococcygeal, pericardial and mediastinal teratomas, the majority are considered unresectable during intrauterine life [21–24]. Thus, prenatal management focuses mainly on alleviating secondary complications such as fetal cardiac failure, hydrops and preterm delivery [20, 25–27]. Large intracranial tumors can cause numerous complications that can affect the fetus and the mother. The most ominous complications include hydrocephalus, intracranial hemorrhage, and very large head size, which can cause uterine rupture, or severe dystocia from cephalopelvic disproportion [28–30]. Highly vascular tumors can result in high-output fetal heart failure and nonimmune hydrops, with a risk for the development of maternal mirror (Ballantyne) syndrome [31–33]. Pregnancy management options for intracranial tumors include termination or continuation of the pregnancy, and this decision usually involves multidisciplinary counseling with the extremely valuable contribution of detailed and accurate imaging. In the next sections of this article we describe and illustrate the common imaging characteristics of congenital brain tumors diagnosed in utero.

## Intracranial teratoma

Teratomas are germ cell tumors and the most frequent type of congenital brain tumor diagnosed prenatally [1, 5, 9, 34, 35]. Many are histologically benign and they generally contain both mature components from all three germ layers as well

**Table 1** Differential diagnosis of fetal brain masses based on location

| Location | Tumor |
|---|---|
| Suprasellar | Teratoma, astrocytoma, craniopharyngioma, lipoma, hypothalamic hamartoma, sublobar dysplasia |
| Supratentorial hemispheric | Astrocytoma, atypical teratoid/rhabdoid tumor, other embryonal tumors, ependymoma, giant subcortical heterotopia, intracranial hemorrhage |
| Posterior fossa | Medulloblastoma, atypical teratoid/rhabdoid tumor, other embryonal tumors, ependymoma, intracranial hemorrhage |
| Intraventricular | Choroid plexus papilloma, choroid plexus carcinoma, subependymal giant cell astrocytoma, intracranial hemorrhage |
| Pineal/tectal | Tectal hamartoma, teratoma, lipoma, pineocytoma, pineoblastoma |
| Peripheral/extra-axial | Meningioma, mesenchymal tumors, hemangiopericytoma, hemangioma, extra-axial hemorrhage |
| Multi-compartment or too large to localize | Teratoma, atypical teratoid/rhabdoid tumor, glioblastoma multiforme, other embryonal tumors |

**Table 2** Tumor predisposition syndromes

| Syndromes | Brain tumor |
|---|---|
| Li–Fraumeni | Glioblastoma |
| Cowden | Dysplastic gangliocytoma cerebellum, i.e. Lhermitte–Duclos disease |
| Turcot | Medulloblastoma and glioblastoma |
| Gorlin | Medulloblastoma |
| Rhabdoid predisposition syndrome | ATRT, medulloblastoma, choroid plexus tumors and former PNET |
| Neurofibromatosis 1 | Astrocytoma |
| Neurofibromatosis 2 | Vestibular, spinal root schwannomas, meningiomas and spinal cord–brainstem ependymomas |
| Tuberous sclerosis complex | Subependymal giant cell astrocytoma |
| Von Hippel–Lindau | Hemangioblastoma |
| Ciliopathies (Pallister–Hall, oro-facial-digital syndrome Type VI) | Hypothalamic hamartoma |

*ATRT* atypical teratoid/rhabdoid tumors, *PNET* primitive neuroectodermal tumor

as immature neuroglial elements [8, 36, 37]. The tumor is usually detected on prenatal US, with an average gestational age at diagnosis of 27 weeks [4, 38, 39]. Fetal MRI further characterizes important details of lesion morphology and location. Intracranial teratoma usually presents as a very large heterogeneous mass, often with more aggressive MR appearance than that seen for postnatal teratomas. The presence of intralesional fat, which is almost pathognomonic for teratomas, is unfortunately difficult to detect with certainty by prenatal imaging. Morphological heterogeneity reflects the complex composition of the tumor and usually indicates a mature, more benign histology (Fig. 1). Mature teratomas more often contain cystic components, calcification/mineralization and fat; immature, malignant teratomas are usually solid and more homogeneous (Fig. 2), although malignant lesions often grow rapidly and can develop necrotic foci and hemorrhage [4, 9, 34]. Most are centrally located; larger lesions tend to occupy more than one cranial fossa, resulting in significant destruction of cerebral tissue. Rapidly growing intracranial teratomas can also destroy the cranium, leading to devastating outcomes [28, 29, 39, 40]. A subset of intracranial teratomas presents with both intra- and extracranial components (Fig. 3). In such cases, the tumor might extend into the face and through the skull base into the oropharyngeal and neck regions, although the precise site of origin can be difficult to discern [30]. For these tumors, the outcome is suboptimal because complete postnatal surgical resection cannot be achieved. Differential diagnoses include craniopharyngiomas, hypothalamic hamartomas and sublobar heterotopias [31].

Large intracranial teratomas are known to cause hydrocephalus, intracranial hemorrhage, and rapidly increasing head size (Fig. 4). In extreme cases, this can result in spontaneous rupture of the fetal head during delivery, and uterine rupture. Severe dystocia from cephalopelvic disproportion can be a dangerous complication during labor [28–30]. High-output fetal heart failure and nonimmune hydrops can

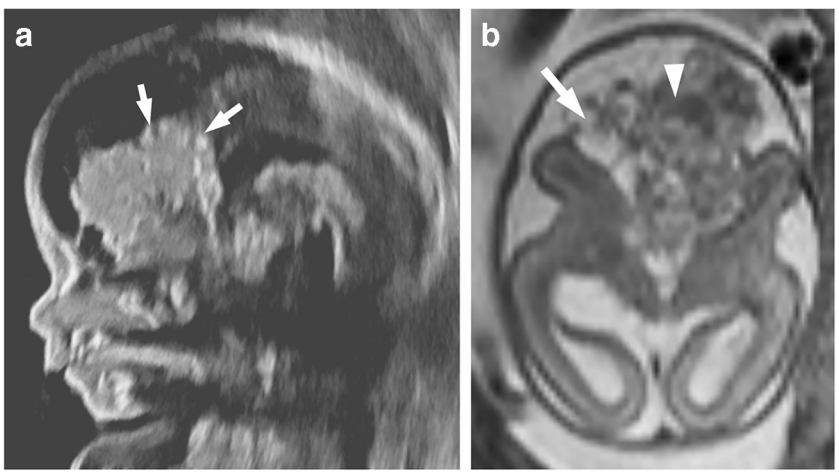


**Fig. 1** Intracranial benign teratoma in a 21-week fetus. **a** Fetal sagittal ultrasound (US) image shows a large heterogeneous midline mass with internal calcifications (*arrows*). **b** Fetal axial MR half-Fourier acquisition single-shot turbo spin-echo (HASTE) image shows that the lesion is multilobulated, with cystic (*arrow*) and solid (*arrowhead*) components. The imaging features are indicative of benign mature teratoma

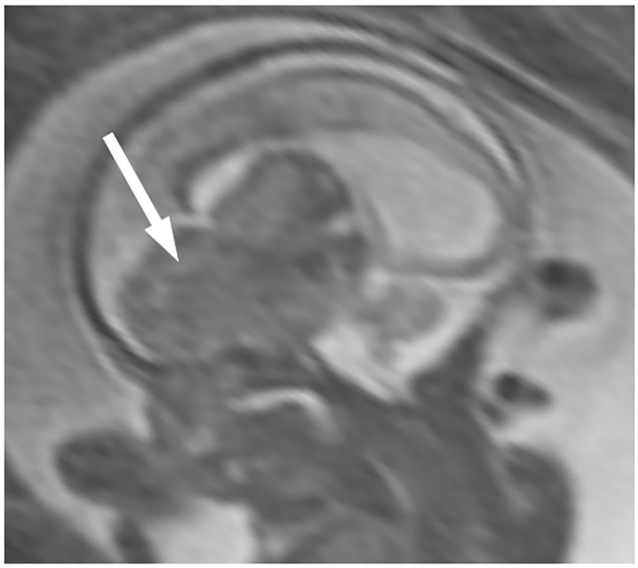

**Fig. 2** Intracranial malignant teratoma in a 25-week fetus. Fetal MR sagittal 2-D true fast imaging with steady-state precession (TrueFISP) image shows solid hypointense midline mass (*arrow*), with the imaging features indicative of immature malignant teratoma

complicate vascular teratomas and lead to maternal seizures and eclampsia, known as mirror syndrome [31–33]. The prognosis for prenatally diagnosed intracranial teratomas is generally poor, with a significantly increased risk of in utero demise and a survival rate of less than 10% for neonates, depending on the time of diagnosis and size of the teratoma [41, 42].

Pregnancy management options include termination or continuation of the pregnancy with multidisciplinary counseling. Available medical (induction of labor) or surgical (dilation and evacuation) termination methods should be discussed. Decompression of the fetal skull via cephalocentesis under US guidance might be required to optimize maternal safety prior to uterine evacuation, regardless of method or timing of delivery [43].

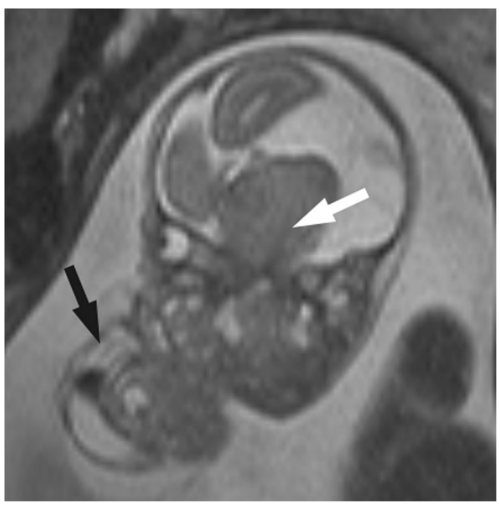

**Fig. 3** Intracranial teratoma with extracranial component in a 21-week fetus. Fetal MR sagittal 2-D true fast imaging with steady-state precession (TrueFISP) image shows heterogeneous lesion with solid intracranial (*white arrow*) and complex extracranial (*black arrow*) components

**Fig. 4** Gigantic intracranial teratoma in a 24-week fetus. Fetal MR sagittal half-Fourier acquisition single-shot turbo spin-echo (HASTE) image shows very large heterogeneous lesion, causing severe enlargement of the fetal head and almost complete replacement of the fetal brain by tumor

Maternal health and long-term well-being are very important considerations, particularly in cases of rapidly growing, rapidly expanding fetal intracranial teratomas. If the parents opt to continue the pregnancy, serial US scans with maternal–fetal medicine surveillance to monitor growth of the teratoma are recommended. The frequency of interval scans varies 1–4 weeks, or even multiple times per week, depending on the pace of tumor growth, which can be quite considerable in a short period of time. The goal is to achieve a gestational age that is term or near term. Caesarean delivery at a facility with available experts in neonatal subspecialties including high-level neonatology care, neurosurgery, plastic surgery and otolaryngology as well as neonatal palliative care might be required.

## Astrocytoma

Astrocytomas are the second most frequent congenital brain tumor, representing 18–47% of all primary neoplasms affecting the fetal brain [5, 6, 9]. They are composed of glial cells (astrocytes) of varying degrees of differentiation. Congenital astrocytomas usually involve the cerebral hemispheres, optic nerve or thalamus. The most common fetal astrocytic tumor is the congenital glioblastoma multiforme (GBM), but other

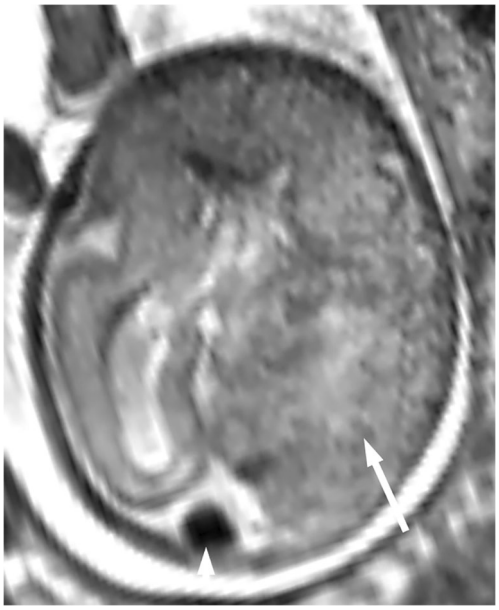

**Fig. 5** Malignant glioblastoma multiforme (GBM) in a 27-week fetus. Fetal MR axial half-Fourier acquisition single-shot turbo spin-echo (HASTE) image shows large solid hypervascular hemorrhagic mass in the left hemisphere (*long arrow*). The lesion causes midline shift and marked dilation of the venous sinus (*short arrow*). Diagnosis of GBM was confirmed on extensive postnatal genetic testing

variants include low-grade astrocytoma, anaplastic astrocytoma and desmoplastic infantile astrocytoma [44, 45]. Most fetal astrocytomas present as a large supratentorial mass that causes shift of midline structures, obstructive hydrocephalus, and increased head circumference [4, 5, 45].

Despite the aggressive imaging features of congenital GBMs, including ill-defined tumor margins and hemorrhage (Fig. 5), these tumors tend to show adequate response to combined resection and chemotherapy, and the prognosis is more favorable compared to that in pediatric and adult GBMs [46, 47].

The genetic and molecular alterations of congenital GBMs are heterogeneous. In a small case series by Gilani et al. [46], three of seven cases showed *ALK* fusions, one case showed *ROS1* fusion and one case showed somatic mutations in *TSC22D1* and *DGCR6* genes. The characteristic alterations of adult GBMs (i.e. *EGFR* amplification and *PTEN* mutation) or pediatric and adolescent GBMs (mutations of Histone 3 genes or *TP53*) are uncommon [46, 48, 49].

Prenatal low-grade gliomas frequently involve the hypothalamus and optic chiasm. These appear as focal suprasellar lesions without aggressive features. Glial tumors are most often detected at the end of the third trimester, later in gestation than other congenital brain tumors [4, 45]; however, they can grow very rapidly. The survival rates range from 20% for high-grade to 90% for low-grade lesions. Overall, the average survival rate is 46% [45]. Pregnancy management options for large hemorrhagic glial tumors are similar to those in intracranial teratomas. If continuation of pregnancy is chosen, serial scans to monitor the rate of tumor growth and multidisciplinary counseling and delivery planning are mandatory.

A distinct subtype of glial tumors is the benign subependymal giant cell astrocytoma (SEGA), also known as subependymal mixed-cell tumor. This lesion is typically located at the foramen of Monro (Fig. 6) and is associated with tuberous sclerosis complex (TSC) in 50% of cases. Most often the diagnosis of TSC is suspected following detection of multiple cardiac rhabdomyomas on prenatal US (Fig. 6). These lesions are known to be associated with TSC in greater than 90% of cases [50, 51]; therefore, their detection necessitates a thorough search for additional cerebral and renal

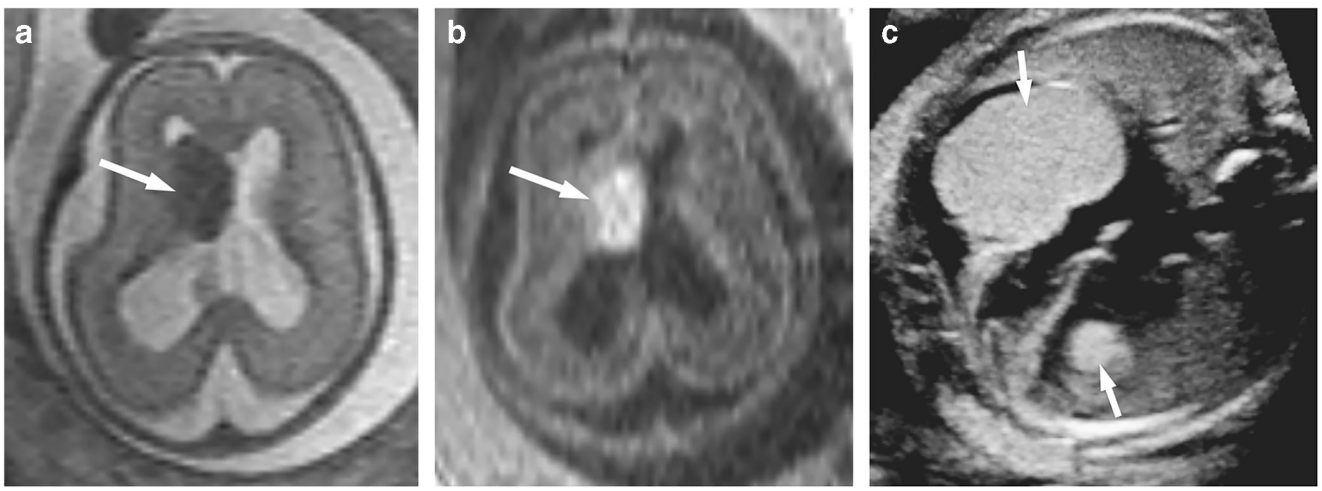


**Fig. 6** Subependymal giant cell astrocytomas (SEGA) in a 22-week fetus with tuberous sclerosis complex (TSC). **a**, **b** Fetal MR axial half-Fourier acquisition single-shot turbo spin-echo (HASTE) (**a**) and axial T1-W (**b**) images show typical location and signal characteristics of SEGA, demonstrating a solid intraventricular mass (*arrows*) at the right foramen of Monro, with T2-hypointense and T1-hyperintense signal. **c** Fetal US cardiac four-chambers view in the same fetus shows solid, uniformly echogenic intracardiac rhabdomyomas (*arrows*), a typical finding in fetuses with TSC

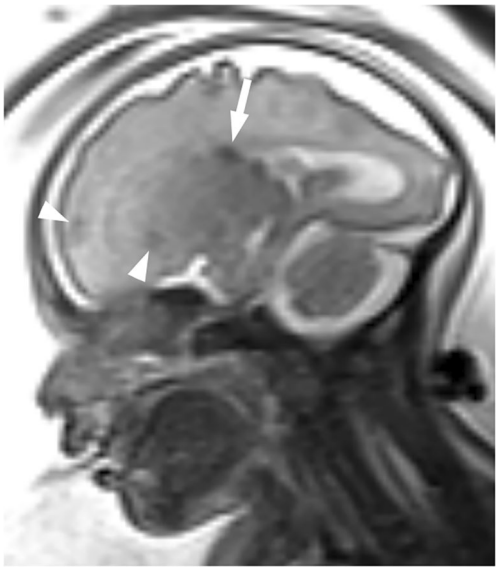

**Fig. 7** Additional cerebral manifestations in a 28-week fetus with tuberous sclerosis complex (TSC). Fetal MR sagittal axial half-Fourier acquisition single-shot turbo spin-echo (HASTE) image shows additional typical cerebral stigmata of tuberous sclerosis: cortical/subcortical tubers (*arrowheads*) and periventricular heterotopia (*arrow*)

lesions that are typical of this disease. Cortical tubers, radiating dysplastic white matter tracts, periventricular subependymal nodules (Fig. 7) and renal lesions (angiomyolipomas) might be demonstrated. The imaging findings of cortical tubers can overlap with those of other congenital brain tumors and, thus, should be included in the differential diagnosis for congenital brain tumors. SEGA can cause obstructive hydrocephalus because of its location at the foramen of Monro. This results in an overall survival rate of 71% and an increased frequency of fetal death [50].

## Choroid plexus tumor

The most common prenatal choroid plexus lesion is the choroid plexus cyst (Fig. 8), found in approximately 1–3% of prenatal US examinations [52]. A small percentage of these lesions is associated with Trisomy 18 [53]; therefore, a detailed US evaluation to check for other features of trisomy is indicated. Isolated choroid plexus cysts do not require additional genetic testing because they are benign lesions with no consequences [54]. Choroid plexus tumors are intraventricular and, as the name implies, originate from the choroid plexus. In the World Health Organization (WHO) grading system, they range from low-grade, WHO Grade I, choroid plexus papilloma to the more aggressive WHO Grade III choroid plexus carcinoma. Choroid plexus papillomas are more common in fetuses than in children, representing 5–20% of all congenital brain tumors [5, 8, 34]. Tumors are composed of mature epithelial cells with similar appearance to normal choroid plexus. In young children and fetuses, the more common location of choroid plexus papillomas is the lateral ventricle (80% cases). The fourth ventricle and cerebellopontine cistern locations are usually seen in adults. Choroid plexus papillomas are more frequent in males; however, an increased frequency of choroid plexus papillomas has also been noted in girls with Aicardi syndrome [55]. On the other hand, choroid plexus carcinoma is known to have a high frequency of *TP53* germline mutations and association with Li–Fraumeni syndrome [56, 57].

Hydrocephalus is a common presenting feature, often attributable to variable contributions from cerebrospinal fluid overproduction, mechanical drainage obstruction or hemorrhage [5]. Choroid plexus tumors usually demonstrate a frondlike appearance and rich vascularity [58]. Unfortunately, no reliable imaging features distinguish choroid plexus papilloma from choroid plexus carcinoma prenatally (Figs. 9 and 10). Choroid plexus hemorrhage can mimic or mask an underlying choroid plexus tumor. Total postnatal resection is possible for 96% of papillomas and for 61% of carcinomas. The prognosis is widely variable between the two forms, with a reported 5-year survival rate of approximately 100% for papillomas and 40% for carcinomas [59]. Surgical procedures are associated with significant operative morbidity and mortality from uncontrolled bleeding. Nevertheless, a

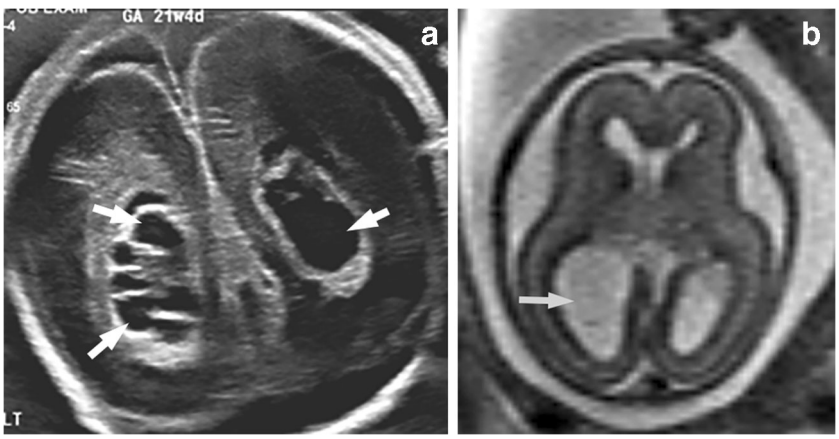


**Fig. 8** Choroid plexus cysts in two fetuses. **a** Coronal US in a 23-week fetus shows multiple bilateral choroid plexus cysts of different sizes (*arrows*). **b** MR axial half-Fourier acquisition single-shot turbo spin-echo (HASTE) image in a 21-week fetus shows a large cyst filling the right ventricular atrium (*arrow*), causing asymmetrical ventriculomegaly

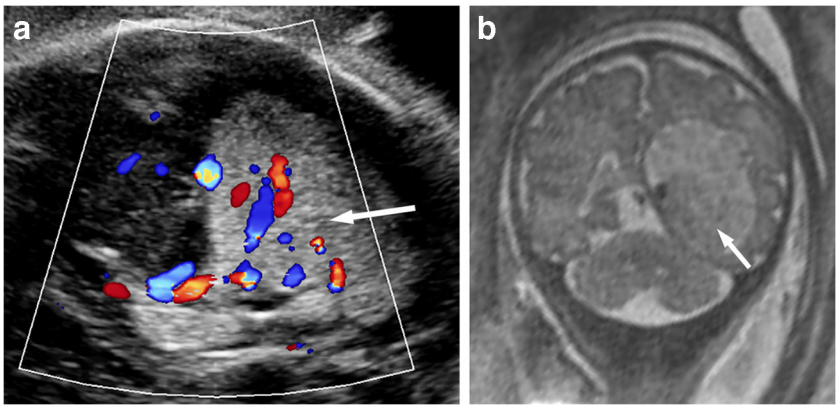


**Fig. 9** Choroid plexus papilloma in a 36-week fetus. **a**, **b** Fetal coronal US with color Doppler (**a**) and fetal MR coronal half-Fourier acquisition single-shot turbo spin-echo (HASTE) (**b**) images show a hyperechoic, vascular, heterogeneous intraventricular mass (*arrow*), expanding the ventricle

final diagnosis of the choroid tumor nature can be accurately confirmed postnatally.

## Medulloblastoma

Medulloblastomas are embryonal tumors that represent 15–20% of all brain tumors in children [58]. Most congenital medulloblastomas are diagnosed postnatally according to several perinatal series [6, 8, 9, 14, 34]. In the last revision of the World Health Organization classification of tumors of the central nervous system from 2016, medulloblastomas were reorganized according to their histology and genetic profiles using a more integrated approach that permits a more comprehensive genotype–phenotype correlation [60]. As a side note, other embryonal tumors also underwent important changes in their classification, including removal of the term primitive neuroectodermal tumor, or PNET, from the diagnostic lexicon [60].

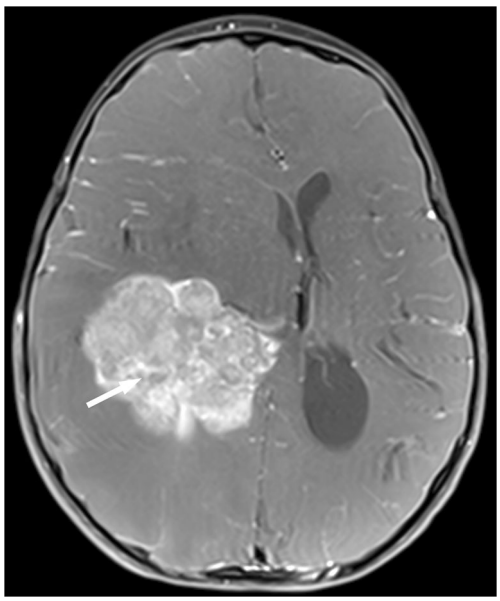

**Fig. 10** Choroid plexus carcinoma in a 7-day-old boy. Axial post-gadolinium T1-W MR image with fat suppression shows an enhancing heterogeneous mass in the right lateral ventricle (*arrow*) with ill-defined margins, causing midline shift

In the updated classification, medulloblastomas are classified into four molecular and five histological subgroups. The most common molecular subgroups in young children are sonic hedgehog and Group 3 [61]. Medulloblastoma with extensive nodularity is a rare histological variant that occurs in infants and young children and is related to *SHH* activation. On MRI, medulloblastomas with extensive nodularity are predominantly solid and hypercellular, with restrictive diffusivity and hypointense T2 signal (Fig. 11). Contrast enhancement is variable on postnatal follow-up, with a tendency to show a pattern of marked multinodular enhancement (Fig. 11). Although most medulloblastomas with extensive nodularity involve the vermis, they also present as diffuse superficial lesions arising from the cerebellar surface. Final diagnosis is usually confirmed by postnatal imaging, and histopathological and molecular evaluation. Medulloblastomas with extensive nodularity have better prognosis than other medulloblastoma variants and sometimes respond to chemotherapy alone [5, 14].

## Atypical teratoid/rhabdoid tumor

Atypical teratoid/rhabdoid tumors (ATRTs) are aggressive WHO Type IV embryonal tumors with median age at presentation of 2–4 years. Cerebrospinal fluid dissemination is common, with approximately 20–30% of cases at presentation. The genetic hallmark is mutation in the *SMARCB1* tumor suppressor gene on chromosome 22q that codes for a subunit (INI1) of the SWI/SNF chromatin remodeling complex. The histological hallmark is the presence of rhabdoid cells. On imaging, these tumors frequently present as large heterogeneous masses with solid, cystic and necrotic components located in different compartments (supra- and infratentorial, intraventricular, pineal or suprasellar). Because of their high cellularity, MRI characteristics are similar to those in medulloblastomas (Fig. 12). One distinguishing feature is that

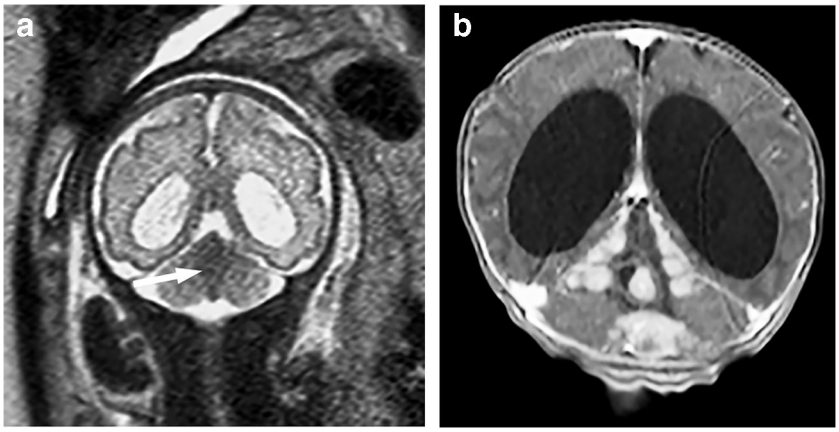


**Fig. 11** Medulloblastoma. **a** MR coronal half-Fourier acquisition single-shot turbo spin-echo (HASTE) image in a 31-week fetus shows subtle T2 hypointensity in the posterior fossa (*arrow*), which effaces the fourth ventricle. The lesion demonstrated restricted diffusion (not shown). **b** Postnatal MR follow-up coronal post-gadolinium T1-W image with fat suppression shows multinodular enhancement in the posterior fossa, which is a typical pattern of medulloblastoma with extensive nodularity

ATRTs often demonstrate rapid growth compared to medulloblastomas and approximately one-third of these tumors show cerebrospinal fluid dissemination at the time of presentation on postnatal imaging. A prompt and correct diagnosis of

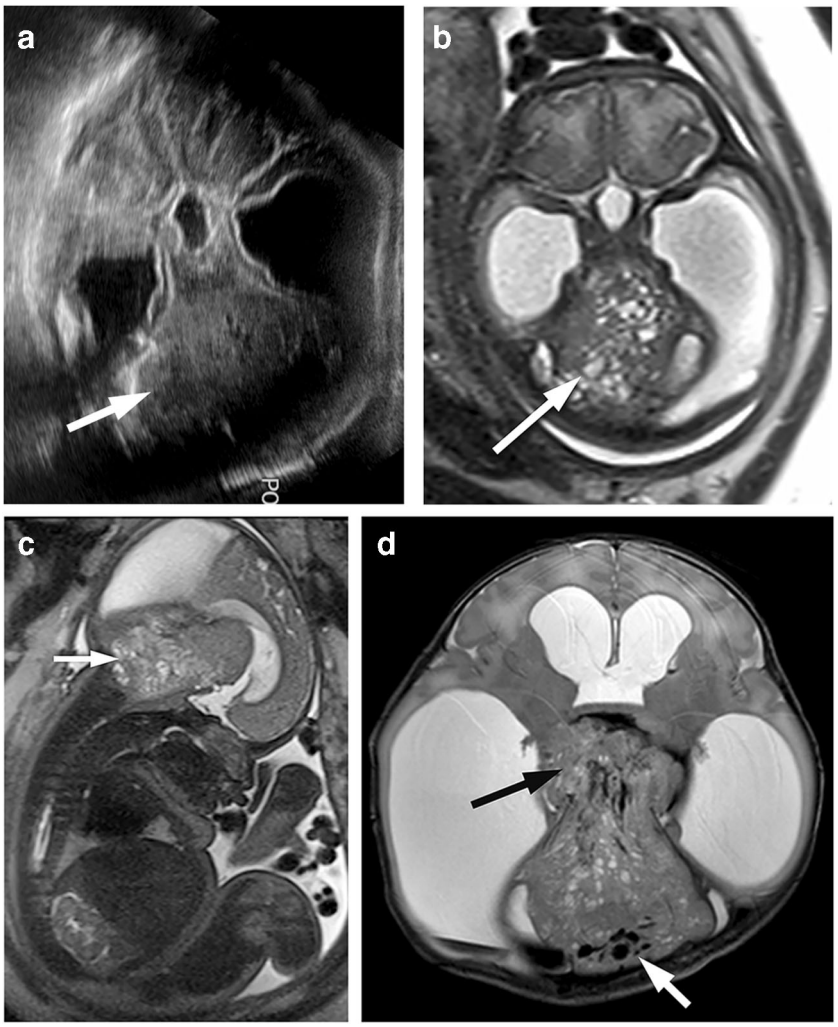


**Fig. 12** Atypical teratoid/rhabdoid tumor (ATRT) **a**, **b** Fetal axial US at 35 weeks 3 days (**a**) and fetal MR axial half-Fourier acquisition single-shot turbo spin-echo (HASTE) at 35 weeks 5 days (**b**) images show severe hydrocephalus and a large heterogeneous tumor in the posterior fossa (*arrow*). **c** Fetal MR sagittal HASTE image shows involvement of the brainstem and thalamus (*arrow*). **d** Postnatal MR axial T2-weighted image (at 1 day old) shows interval tumor growth with increased thalamic invasion (*black arrow*) and development of intratumoral hemorrhage (*white arrow*)

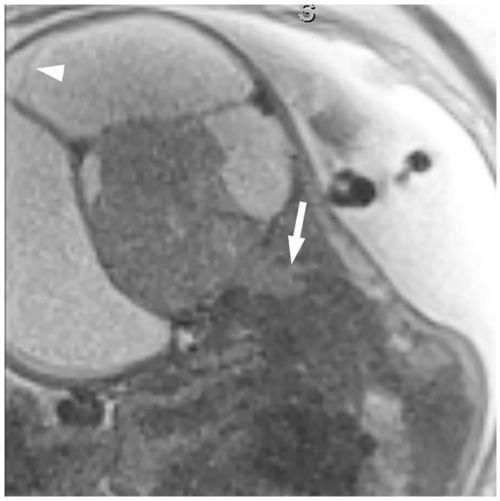

**Fig. 13** Ependymoma. MR coronal half-Fourier acquisition single-shot turbo spin-echo (HASTE) image in a 37-week fetus shows a large tumor in the posterior fossa, extending into the spinal canal (*arrow*). The lateral ventricles (*arrowhead*) and third ventricle (not shown) are markedly dilated and contribute to significant distortion of the normal anatomy. Tumor extension into the spinal canal is suggestive of ependymoma. The diagnosis was confirmed postnatally

ATRTs is crucial because radical and aggressive therapies are required to potentially alter their natural progression [58].

## Craniopharyngioma

Craniopharyngioma is a WHO Grade I benign tumor located in the sella turcica and suprasellar region. While craniopharyngioma is the most common pediatric tumor to occur in the parasellar region, it rarely occurs in the perinatal period, representing 5.6% of all fetal and neonatal tumors [6, 8, 62–66]. Fetuses and neonates with large craniopharyngiomas generally have poor prognosis and low survival rate [6, 8]. It is difficult to distinguish craniopharyngiomas from other solid suprasellar masses, such as other tumors (teratoma or chiasmatic–hypothalamic astrocytomas) or malformations (hypothalamic hamartomas or the even rarer sublobar heterotopia) because of their often similar imaging appearance [31].

## Ependymoma

Ependymomas represent 2–3% of all congenital brain tumors, and approximately 30% of all pediatric ependymomas are diagnosed in children younger than 3 years [11]. Fetal ependymomas are rare. The first reported case was incidentally discovered during the autopsy of a fetus with Down syndrome [12]. From the different ependymoma subtypes, the anaplastic form, a high-grade WHO Grade III lesion, is the most frequently encountered. The tumor is composed of poorly differentiated neuroepithelial cells with high mitotic activity. They usually present as large multilobulated supratentorial or infratentorial masses with intrinsic calcifications (Fig. 13). The lesions might protrude into the posterior fossa and into the spinal canal. Complete or near-complete tumor resection followed by adjuvant therapy is the treatment of choice.

In neonates and young children, because of a wide variety of patient- and therapy-related issues, the application and response to standard treatment protocols are more limited. For these reasons, fetal ependymomas are associated with overall poor prognosis [10].

## Other masses and tumor-like conditions

### Hypothalamic hamartoma

Hypothalamic hamartoma is a benign lesion that is a characteristic but not universal feature of oral–facial–digital syndrome Type VI, a.k.a. Varadi–Papp syndrome, and is seen in other ciliopathies including Pallister–Hall syndrome, hydrolethalus syndrome and short rib polydactyly syndrome.

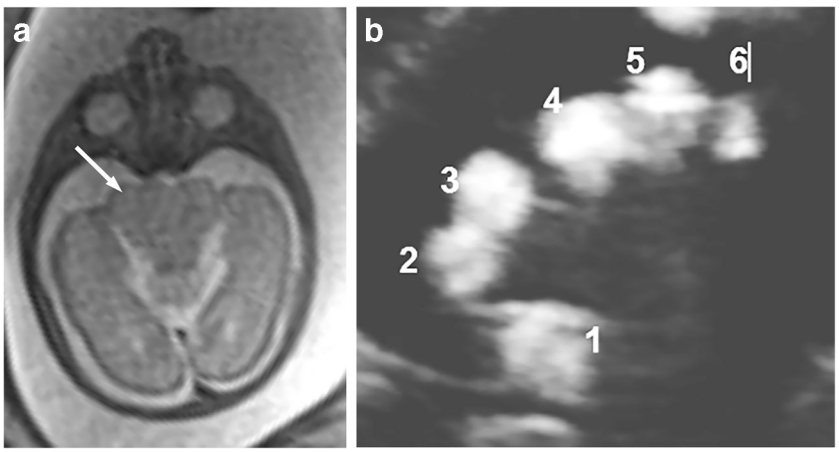


**Fig. 14** Hypothalamic hamartoma in a 28-week fetus with Pallister–Hall syndrome. **a** Fetal MR axial half-Fourier acquisition single-shot turbo spin-echo (HASTE) image shows suprasellar homogeneous isointense mass at the midline (*arrow*), confirmed to be hamartoma. **b** Fetal hand US in the same fetus shows polydactyly, which is one of the typical findings in patients with this syndrome

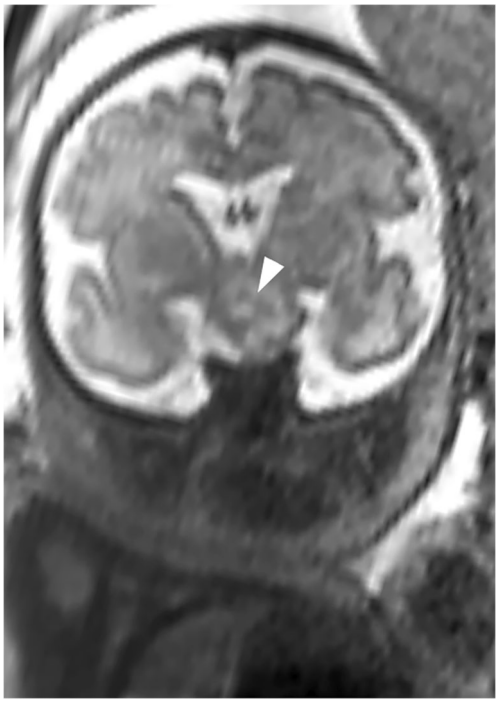

**Fig. 15** Sellar sublobar dysplasia in a 32-week fetus. Fetal MR coronal half-Fourier acquisition single-shot turbo spin-echo (HASTE) image shows a midline mass in the suprasellar cistern consisting of dysplastic brain tissue with visible gray (*arrowhead*) and white matter

Thus, a thorough search for possible extracranial manifestations of these conditions should be performed. In cases of Pallister–Hall syndrome, these anomalies include polydactyly, syndactyly, imperforate anus, growth restriction, and genital anomalies (e.g., hydrometrocolpos secondary to vaginal atresia, micropenis, hypoplastic scrotum, cryptorchidism) (Fig. 14) [67, 68].

## Sublobar dysplasia

Sublobar dysplasia is a rare malformation of cortical development usually localized in the cerebral hemispheres but also involving the suprasellar region [69]. The lesion presents as a mass-like focus of disorganized gray and white matter separated from the remainder of the affected lobe or cerebral hemisphere by a deep infolding of cortex (Fig. 15). Callosal dysgenesis, vermian hypoplasia and venous malformations are sometimes associated [69].

## Pineal/tectal mass

Pineal/tectal plate lesions represent a heterogeneous collection of tumors and congenital malformations; they are very rarely detected prenatally [4]. Their exact origin and nature is difficult to define because their imaging characteristics have similar features. Diffuse enhancement suggestive of the neoplastic nature of pineal lesions can be seen on postnatal imaging; however, no contrast administration is used for prenatal imaging and reliable distinction between the fetal pineal tumor and tectal plate hamartoma can be difficult. The most common prenatal pineal masses are teratoma and lipoma. They demonstrate fat signal characteristics on MRI, although fetal fat is often poorly discernable on prenatal imaging. Other congenital pineal tumors that can occur in utero are benign parenchymal pineocytoma (Fig. 16) and malignant pineoblastomas. These lesions, regardless of their etiology, can manifest as a very uncommon cause of fetal aqueductal stenosis and hydrocephalus. Tectal hamartoma can appear identical to pineal tumor on prenatal imaging but does not cause hydrocephalus and does not enhance on postnatal imaging. Very infrequently, a hamartomatous lesion involving a lower portion of the brainstem (Fig. 17) occurs in utero.

## Gray matter heterotopia

Gray matter heterotopias are common malformations of cortical development that result from premature arrest of neuronal migration. These ectopic neurons have variable morphologies and can be localized in the subcortical, subependymal regions

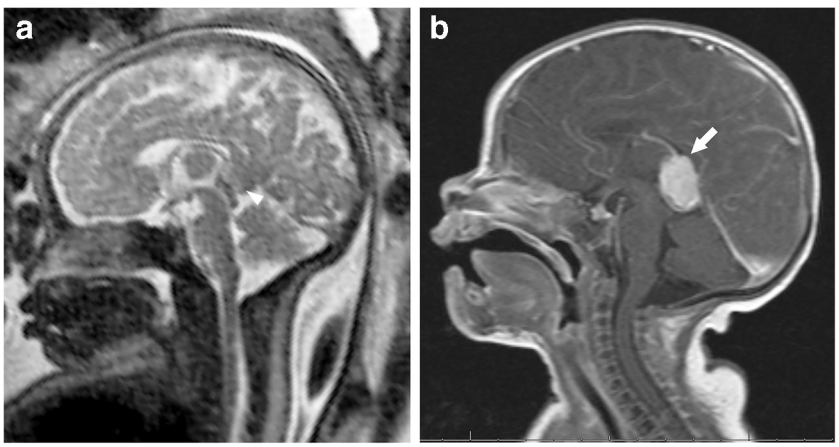


**Fig. 16** Pineocytoma. **a** Fetal MR sagittal half-Fourier acquisition single-shot turbo spin-echo (HASTE) image in a 36-week fetus shows an isointense pineal mass (*arrowhead*). **b** Postnatal follow-up MRI at 3 weeks of age. Sagittal post-gadolinium T1-W MR image shows an avidly and homogeneously enhancing pineal tumor (*arrow*) with no restricted diffusion (not shown), confirmed to be pineocytoma

**Fig. 17** Brainstem hamartoma in a 34-week fetus. Fetal MR sagittal half-Fourier acquisition single-shot turbo spin-echo (HASTE) image shows a small focus of isointense tissue (*arrow*) extending from the tectal plate, with similar size and imaging features of cerebral tissue on postnatal follow-up (not shown)

or central white matter (band heterotopia). When lesions present as large conglomerates, they can mimic tumors (Fig. 18). Depending on the extent of malformation and presence/absence of associated anomalies, these children can be asymptomatic or develop intellectual disability or epilepsy.

## Intracranial lipoma

Intracranial lipomas are rare benign and slow-growing congenital hamartomatous conditions. They represent approximately 0.5–1.0% of all intracranial tumors and are thought to result from abnormal reabsorption of the primitive meninx at 8–10 weeks of embryonic development [70]. The majority are located at or about the midline (80–90%), favoring the pericallosal region and quadrigeminal cistern. Other locations, in order of decreasing frequency, include the suprasellar/interpeduncular cistern, cerebellopontine angle and sylvian cisterns [71]. Most prenatally diagnosed intracranial lipomas are found in the pericallosal region (Figs. 19 and 20). As formation of the corpus callosum begins at the genu during the 11th week of gestation and, thus, overlaps with reabsorption of the primitive meninx, it is not surprising that pericallosal lipomas are associated with abnormal development of the corpus callosum [72].

Two subtypes of pericallosal lipomas have been described. The tubulonodular type is more frequent, round or oval in shape, located close to the genu, and has a higher association with craniofacial anomalies and callosal agenesis. The curvilinear type is thin and elongated and tends to be located posteriorly around the splenium. It has a higher association with hypoplastic or dysplastic corpus callosum and a lower frequency of associated anomalies [73]. In a systematic review of 49 published cases of prenatally diagnosed pericallosal lipomas, the mean gestational age at diagnosis was 29.6 weeks, hypoplastic corpus callosum was present in 79.2% of curvilinear lipomas, partial or complete agenesis of the corpus callosum was found in 76.5% of tubulonodular lipomas, and syndromic association was observed with Pai syndrome in 3 cases and Goldenhar syndrome in another 3 [72]. Neurologic evaluation was

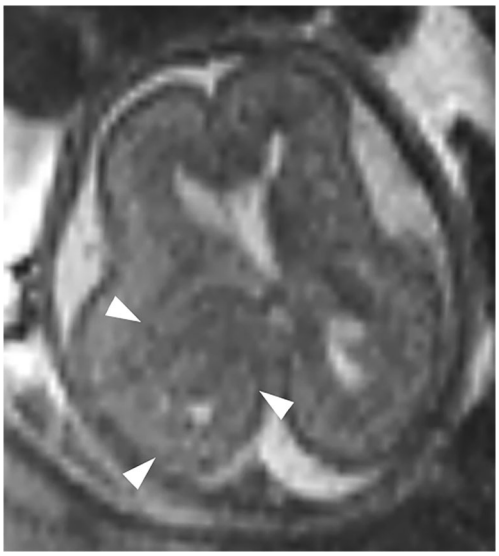

**Fig. 18** Giant subcortical heterotopia in a 24-week fetus. Fetal MR axial half-Fourier acquisition single-shot turbo spin-echo (HASTE) image shows a large mass-like heterogeneous thickening in the right hemisphere (*arrowheads*)

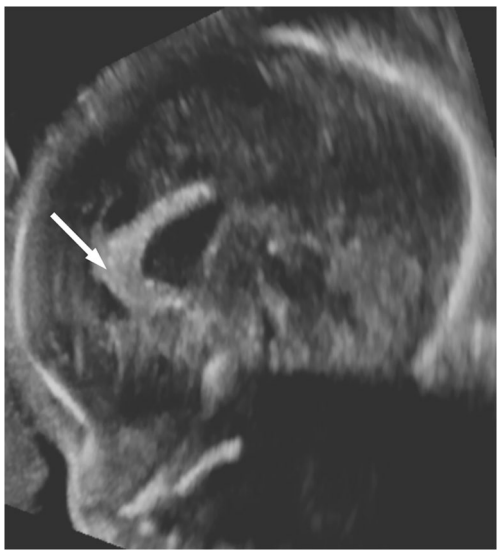

**Fig. 19** Intracranial lipoma in a 21-week fetus. Fetal sagittal US shows hyperechoic interhemispheric mass (*arrow*), which was T1 hyperintense and poorly discernable on half-Fourier acquisition single-shot turbo spin-echo (HASTE) MR imaging (not shown). The corpus callosum was underdeveloped

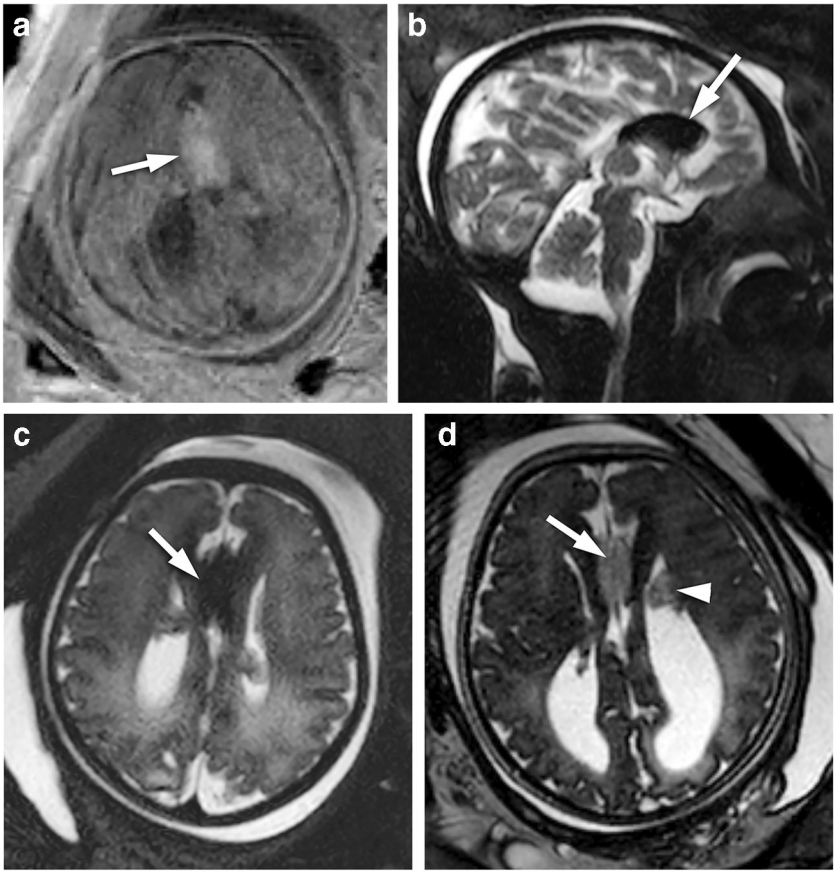


**Fig. 20** Intracranial lipoma in a 37-week fetus. **a**–**d** Axial T1-W fast field echo imaging (**a**), sagittal T2-weighted (**b**), axial T2-weighted (**c**) and axial balanced turbo field echo (**d**) fetal MRI sequences show a well-circumscribed tubular lesion at midline (*arrow*) with a few scattered nodules at the ventricular margins (*arrowhead*, **d**)

normal in 92% of the cases (mean postnatal follow-up age 36.3 months), with tubulonodular lipomas presenting more frequently with neurologic anomalies [72]. Lipomas are slow-growing lesions with generally good prognosis. Indeed, most intracranial lipomas are asymptomatic. Possible clinical manifestations include seizures for lipomas localized to the Sylvian region, as well as hearing loss, tinnitus, dizziness and vertigo for cerebellopontine tumors [70]. For pericallosal lipomas, outcome is also determined by the degree of associated malformation of the corpus callosum and severity of associated anomalies, particularly for syndromic cases.

## Intracranial hemorrhage

Intracranial hemorrhage might be present with imaging findings that resemble a brain tumor, i.e. a mass-like lesion with heterogeneous signal intensity by fetal MRI, varying echogenicity by US, and mass effect upon adjacent brain structures. Conversely, a brain tumor with hemorrhagic features can mimic intracranial hemorrhage at first glance [74, 75]. When intracranial hemorrhage mimics a tumor, it is seen by US as an intracranial mass, at first hyperechogenic, changing over the course of days to a lesion with hypoechoic core and hyperechogenic rim as hemoglobin degrades. An important finding on US is the absence of vascularization by color Doppler within the organized clot [74, 75]. The appearance on fetal MRI varies depending on the stage of degradation of hemoglobin products, but in most cases lesions present with hyperintense signal on T1, hypointense signal on T2, and blooming artifact on gradient echo sequences. Most cases of prenatal intracranial hemorrhage originate in the germinal matrix (approximately 67%), followed by the cerebral or cerebellar parenchyma, choroid plexus, and subdural and subarachnoid spaces (Fig. 21). Long-term sequelae include subependymal as well as porencephalic cysts in case of involvement of the brain parenchyma. In more than 50% of the cases no cause is found; the remaining causes include maternal conditions, obstetric complications and fetal disorders. These include umbilical/placental anomalies; maternal trauma, infection, coagulopathy/use of anticoagulants, substance abuse; fetal–neonatal alloimmune thrombocytopenia; gene mutations, e.g., *COL4A1* associated with hereditary parenchymal hemorrhage and porencephaly; fetal coagulopathies,

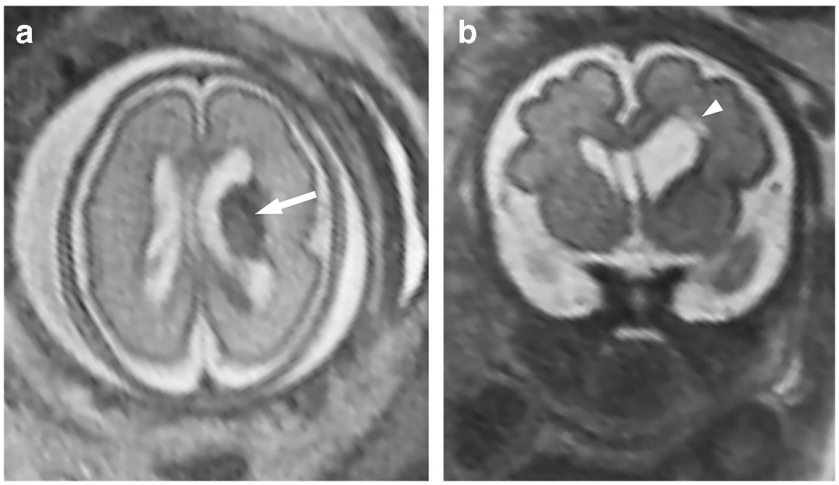


**Fig. 21** Grade IV germinal matrix hemorrhage. **a** Fetal MR axial half-Fourier acquisition single-shot turbo spin-echo (HASTE) image in a 25-week fetus shows hypointense periventricular mass (*arrow*) with marked susceptibility, which extends into the adjacent brain parenchyma. **b** Four-week follow-up. Fetal coronal HASTE image shows asymmetrical ventriculomegaly and cystic focal changes (*arrowhead*) indicative of clot lysis and retraction and periventricular leukomalacia (PVL)

i.e. Factor X and Factor V deficiencies; and vascular malformations.

## Conclusion

Teratomas are the most frequent congenital brain tumors diagnosed prenatally, presenting as an aggressive large heterogeneous mass at an average gestational age of 27 weeks. The presence of intralesional fat is almost pathognomonic for teratomas but difficult to detect with certainty by prenatal imaging.

Astrocytomas are the second most common congenital brain tumor. The most common histological subtype is the highly aggressive glioblastoma multiforme, which usually presents as a large supratentorial mass involving the cerebral hemispheres. Low-grade gliomas tend to involve the optic nerve or thalamus and present as suprasellar masses without aggressive features. Subependymal giant cell astrocytomas are typically located in the foramen of Monro and are associated with tuberous sclerosis complex in 50% of cases.

Choroid plexus papillomas and choroid plexus carcinomas are difficult to differentiate by imaging. These are intraventricular tumors with a frondlike appearance and increased vascularity that originate in the lateral ventricle in 80% of cases, are more frequent in males, and commonly present with hydrocephalus.

Less frequent tumors that might be detected in utero include medulloblastomas, atypical teratoid/rhabdoid tumors, ependymomas, craniopharyngiomas and hypothalamic hamartomas. Tumor-like lesions including sublobar dysplasias, heterotopias, lipomas and hemorrhage can mimic neoplasms. Prenatal detection of fetal brain tumors and tumor-like conditions usually requires prenatal or postnatal imaging follow-up to further characterize the lesion, define additional anomalies, plan therapy and guide parental counseling.

### Compliance with ethical standards

**Conflicts of interest** None

## References

1. Milani HJ, Araujo Júnior E, Cavalheiro S et al (2015) Fetal brain tumors: prenatal diagnosis by ultrasound and magnetic resonance imaging. World J Radiol 7:17–21
2. Uysal A, Oztekin O, Oztekin D, Polat M (2005) Prenatal diagnosis of a fetal intracranial tumor. Arch Gynecol Obstet 272:87–89
3. Schlembach D, Bornemann A, Rupprecht T, Beinder E (1999) Fetal intracranial tumors detected by ultrasound: a report of two cases and review of the literature. Ultrasound Obstet Gynecol 14: 407–418
4. Cassart M, Bosson N, Garel C et al (2008) Fetal intracranial tumors: a review of 27 cases. Eur Radiol 18:2060–2066
5. Severino M, Schwartz ES, Thurnher MM et al (2010) Congenital tumors of the central nervous system. Neuroradiology 52:531–548
6. Isaacs H (2002) I. Perinatal brain tumors: a review of 250 cases. Pediatr Neurol 27:249–261
7. Nozaki M, Ohnishi A, Fujimaki T et al (2006) Congenital gemistocytic astrocytoma in a fetus. Childs Nerv Syst 22:168–171
8. Woodward PJ, Sohaey R, Kennedy A, Koeller KK (2005) From the archives of the AFIP: a comprehensive review of fetal tumors with pathologic correlation. Radiographics 25:215–242
9. Isaacs H (2002) II. Perinatal brain tumors: a review of 250 cases. Pediatr Neurol 27:333–342
10. Buetow PC, Smirniotopoulos JG, Done S (1990) Congenital brain tumors: a review of 45 cases. AJNR Am J Neuroradiol 11:793–799
11. Venkatesh I, Kumar S, Mishra S (2015) Anaplastic ependymoma: a rare brain tumor in a neonate. J Clin Neonatol 4:265–267
12. Rickert CH, Göcke H, Paulus W (2002) Fetal ependymoma associated with Down's syndrome. Acta Neuropathol 103:78–81
13. Ermis B, Aydemir C, Taspinar O et al (2006) Congenital medulloblastoma. Arch Dis Child Fetal Neonatal Ed 91:F373

14. Korostyshevskaya AM, Savelov AA, Papusha LI et al (2018) Congenital medulloblastoma: fetal and postnatal longitudinal observation with quantitative MRI. Clin Imaging 52:172–176
15. Diguet A, Laquerrière A, Eurin D et al (2002) Fetal capillary haemangioblastoma: an exceptional tumour. A review of the literature. Prenat Diagn 22:979–983
16. Madsen C, Schroder HD (1993) Congenital intracranial meningioma. APMIS 101:923–925
17. Shekdar K, Feygin T (2011) Fetal neuroimaging. Neuroimaging Clin N Am 21:677–703
18. Korostyshevskaya AM, Prihod'ko IY, Savelov AA, Yarnykh VL (2019) Direct comparison between apparent diffusion coefficient and macromolecular proton fraction as quantitative biomarkers of the human fetal brain maturation. J Magn Reson Imaging 50:52–61
19. Yarnykh VL (2012) Fast macromolecular proton fraction mapping from a single off-resonance magnetization transfer measurement. Magn Reson Med 68:166–178
20. Luks FI, Deprest JA (1993) Endoscopic fetal surgery: a new alternative? Eur J Obstet Gynecol Reprod Biol 52:1–3
21. Takayasu H, Kitano Y, Kuroda T et al (2010) Successful management of a large fetal mediastinal teratoma complicated by hydrops fetalis. J Pediatr Surg 45:e21–e24
22. Merchant AM, Hedrick HL, Johnson MP et al (2005) Management of fetal mediastinal teratoma. J Pediatr Surg 40:228–231
23. Rychik J, Khalek N, Gaynor JW et al (2016) Fetal intrapericardial teratoma: natural history and management including successful in utero surgery. Am J Obstet Gynecol 215:780.e1–780.e7
24. Langer JC, Harrison MR, Schmidt KG et al (1989) Fetal hydrops and death from sacrococcygeal teratoma: rationale for fetal surgery. Am J Obstet Gynecol 160:1145–1150
25. Birnholz JC, Frigoletto FD (1981) Antenatal treatment of hydrocephalus. N Engl J Med 304:1021–1023
26. Bruner JP, Davis G, Tulipan N (2006) Intrauterine shunt for obstructive hydrocephalus — still not ready. Fetal Diagn Ther 21: 532–539
27. Hodges R, De Catte L, Devlieger R et al (2018) Antenatal diagnosis: current status for paediatric surgeons. In: Losty PD, Flake AW, Rintala RJ et al (eds) Rickham's neonatal surgery. Springer, London, pp 63–103
28. Washburne JF, Magann EF, Chauhan SP et al (1995) Massive congenital intracranial teratoma with skull rupture at delivery. Am J Obstet Gynecol 173:226–228
29. Bolat F, Kayaselcuk F, Tarim E et al (2008) Congenital intracranial teratoma with massive macrocephaly and skull rupture. Fetal Diagn Ther 23:1–4
30. Alagappan A, Shattuck KE, Rowe T, Hawkins H (1998) Massive intracranial immature teratoma with extracranial extension into oral cavity, nose, and neck. Fetal Diagn Ther 13:321–324
31. Hirsigk L, Rajderkar D (2016) Fetal intracranial neoplasm — not always a teratoma! J Radiol Imaging 1:14–17
32. Mathias CR, Rizvi C (2019) The diagnostic conundrum of maternal mirror syndrome progressing to pre-eclampsia — a case report. Case Rep Womens Health 23:e00122
33. Braun T, Brauer M, Fuchs I et al (2010) Mirror syndrome: a systematic review of fetal associated conditions, maternal presentation and perinatal outcome. Fetal Diagn Ther 27:191–203
34. Isaacs H (2009) Fetal brain tumors: a review of 154 cases. Am J Perinatol 26:453–466
35. Isaacs H (2013) Brain tumors. In: Tumors of the fetus and infant. Springer, Berlin, pp 163–195
36. Rickert CH (1999) Neuropathology and prognosis of foetal brain tumours. Acta Neuropathol 98:567–576
37. Rickert CH, Probst-Cousin S, Louwen F et al (1997) Congenital immature teratoma of the fetal brain. Childs Nerv Syst 13:556–559
38. Kurishima C, Wada M, Sakai M et al (2012) Congenital brain tumor: fetal case of congenital germ cell intracranial tumor. Pediatr Int 54:282–285
39. Köken G, Yilmazer M, Sahin FK et al (2008) Prenatal diagnosis of a fetal intracranial immature teratoma. Fetal Diagn Ther 24:368–371
40. O'Grady J, Kobayter L, Kaliaperumal C, O'Sullivan M (2012) 'Teeth in the brain' — a case of giant intracranial mature cystic teratoma. BMJ case rep 2012:bcr0320126130
41. Peiró JL, Sbragia L, Scorletti F et al (2016) Management of fetal teratomas. Pediatr Surg Int 32:635–647
42. Kamil D, Tepelmann J, Berg C et al (2008) Spectrum and outcome of prenatally diagnosed fetal tumors. Ultrasound Obstet Gynecol 31:296–302
43. Cavalheiro S, Moron AF, Hisaba W et al (2003) Fetal brain tumors. Childs Nerv Syst 19:529–536
44. Heckel S, Favre R, Gasser B, Christmann D (1995) Prenatal diagnosis of a congenital astrocytoma: a case report and literature review. Ultrasound Obstet Gynecol 5:63–66
45. Isaacs H (2016) Perinatal (fetal and neonatal) astrocytoma: a review. Childs Nerv Syst 32:2085–2096
46. Gilani A, Donson A, Whiteway S et al (2019) HGG-26. Targetable molecular alterations in congenital glioblastoma. Neuro Oncol 21: ii92
47. Patay Z (2016) New concepts in the imaging of pediatric brain tumors: the revival of age-old real estate principles. Curr Radiol Rep 4:32
48. Brat DJ, Shehata BM, Castellano-Sanchez AA et al (2007) Congenital glioblastoma: a clinicopathologic and genetic analysis. Brain Pathol 17:276–281
49. Macy ME, Birks DK, Barton VN et al (2012) Clinical and molecular characteristics of congenital glioblastoma. Neuro Oncol 14: 931–941
50. Isaacs H (2009) Perinatal (fetal and neonatal) tuberous sclerosis: a review. Am J Perinatol 26:755–760
51. Bader RS, Chitayat D, Kelly E et al (2003) Fetal rhabdomyoma: prenatal diagnosis, clinical outcome, and incidence of associated tuberous sclerosis complex. J Pediatr 143:620–624
52. Shah N (2018) Prenatal diagnosis of choroid plexus cyst: what next? J Obstet Gynaecol India 68:366–368
53. Cheng P-J, Shaw S-W, Soong Y-K (2006) Association of fetal choroid plexus cysts with Trisomy 18 in a population previously screened by nuchal translucency thickness measurement. J Soc Gynecol Investig 13:280–284
54. DiPietro JA, Cristofalo EA, Voegtline KM, Crino J (2011) Isolated prenatal choroid plexus cysts do not affect child development. Prenat Diagn 31:745–749
55. Hopkins B, Sutton VR, Lewis RA et al (2008) Neuroimaging aspects of Aicardi syndrome. Am J Med Genet A 146A:2871–2878
56. Tabori U, Shlien A, Baskin B et al (2010) TP53 alterations determine clinical subgroups and survival of patients with choroid plexus tumors. J Clin Oncol 28:1995–2001
57. Liu AK, Hankinson T, Wolff JEA (2018) Choroid plexus tumors. In: Radiation oncology for pediatric CNS tumors. Springer International, Cham, pp 353–363
58. Parmar HA, Pruthi S, Ibrahim M, Gandhi D (2011) Imaging of congenital brain tumors. Semin Ultrasound CT MR 32:578–589
59. Pencalet P, Sainte-Rose C, Lellouch-Tubiana A et al (1998) Papillomas and carcinomas of the choroid plexus in children. J Neurosurg 88:521–528
60. Louis DN, Perry A, Reifenberger G et al (2016) The 2016 World Health Organization classification of tumors of the central nervous system: a summary. Acta Neuropathol 131:803–820
61. Juraschka K, Taylor MD (2019) Medulloblastoma in the age of molecular subgroups: a review. J Neurosurg Pediatr 24:353–363

62. Sosa-Olavarría A, Díaz-Guerrero L, Reigoza A et al (2001) Fetal craniopharyngioma: early prenatal diagnosis. J Ultrasound Med 20: 803–806
63. Kostadinov S, Hanley CL, Lertsburapa T et al (2014) Fetal craniopharyngioma: management, postmortem diagnosis, and literature review of an intracranial tumor detected in utero. Pediatr Dev Pathol 17:409–412
64. Jurkiewicz E, Bekiesińska-Figatowska M, Duczkowski M et al (2010) Antenatal diagnosis of the congenital craniopharyngioma. Polish J Radiol 75:98–102
65. Joó JG, Rigó J, Sápi Z, Timár B (2009) Foetal craniopharyngioma diagnosed by prenatal ultrasonography and confirmed by histopathological examination. Prenat Diagn 29:160–163
66. do Prado Aguiar U, Araujo JLV, Veiga JCE et al (2013) Congenital giant craniopharyngioma. Childs Nerv Syst 29:153–157
67. Kuo JS, Casey SO, Thompson L, Truwit CL (1999) Pallister–Hall syndrome: clinical and MR features. AJNR Am J Neuroradiol 20: 1839–1841
68. Li MH, Eberhard M, Mudd P et al (2015) Total colonic aganglionosis and imperforate anus in a severely affected infant with Pallister–Hall syndrome. Am J Med Genet A 167A:617–620
69. Barkovich AJ, Peacock W (1998) Sublobar dysplasia: a new malformation of cortical development. Neurology 50:1383–1387
70. Yilmaz N, Unal O, Kiymaz N et al (2006) Intracranial lipomas — a clinical study. Clin Neurol Neurosurg 108:363–368
71. Truwit CL, Barkovich AJ (1990) Pathogenesis of intracranial lipoma: an MR study in 42 patients. AJR Am J Roentgenol 155:855–864
72. Prieto LJ, Ruiz Y, Pérez R, De León LJ (2019) Prenatal diagnosis of pericallosal lipoma: systematic review. Eur J Paediatr Neurol 23: 764–782
73. Demaerel P, Van De Gaer P, Wilms G, Baert AL (1996) Interhemispheric lipoma with variable callosal dysgenesis: relationship between embryology, morphology, and symptomatology. Eur Radiol 6:904–909
74. Thankamony A, Harlow FH, Ponnampalam J, Clarke P (2007) Congenital brain tumour mimicking fetal intracranial haemorrhage. J Obstet Gynaecol 27:314–317
75. Emamian SA, Bulas DI, Vezina GL et al (2002) Fetal MRI evaluation of an intracranial mass: in utero evolution of hemorrhage. Pediatr Radiol 32:593–597